Astrophysical images of static boson stars in the Einstein-Friedberg-Lee-Sirlin theory

Pedro L. B. de Sá, Haroldo C. D. L. Junior, Luis C. B. Crispino, Carlos A. R. Herdeiro

18th November 2024

Federal University of Pará
Institute of Exact and Natural Sciencies
Pos-graduate Program of Physics

Summary

Introduction

Introduction

- Boson stars are an example of non-topological solitons. They are supposed to exist in nature as compact objects composed only of bosonic particles.

2. Static boson stars in the Einstein-Friedberg-Lee-Sirlin Theory

The Einstein-Friedberg-Lee-Sirlin model

The Einstein-Friedberg-Lee-Sirlin (E-FLS) model can be utilized to study field configurations influenced by gravity in more realistic theories with symmetry breaking potentials as, for example, the Standard Model. The E-FLS action is given by (Friedberg, 1976):

$$S = \int d^4x\sqrt{-g}\left(\frac{R}{2\kappa^2} - \mathcal{L}_m\right), \tag{1}$$

where the $\mathcal{L}_m$ is given by:

$$\mathcal{L}_m = \frac{1}{2}\nabla_\mu\psi\,\nabla^\mu\psi + \nabla_\mu\Phi\,\nabla^\mu\Phi^* + U(\psi,\Phi), \tag{2}$$

$$U(\psi,\Phi) = m^2\psi^2\left|\Phi\right|^2 + \mu^2\left(\psi^2 - v^2\right)^2, \tag{3}$$

being ψ a self-interacting real scalar field and Φ a complex scalar field. The real and complex scalar fields are coupled through the coupling constant m.

The Einstein-Friedberg-Lee-Sirlin Field Equations

The constant v is the vacuum expectation value of the real scalar field. We also can see that:

$$\text{For } \mu \to \infty, \text{ then } \psi \to v, \tag{4}$$

and the E-FLS theory recovers the Einstein-Klein-Gordon model. The E-FLS field equations are obtained by varying the action with respect to the metric $g_{\mu\nu}$ and the scalar fields ψ and Φ, respectively:

$$R_{\mu\nu} - \frac{1}{2} R g_{\mu\nu} = \kappa^2 T_{\mu\nu}, \tag{5}$$

$$\Box \Phi = m^2 \psi^2 \Phi, \tag{6}$$

$$\Box \psi = 2\psi \left(m^2 \left|\Phi\right|^2 + 2\mu^2 \psi^2 - 2 v^2 \mu^2 \right). \tag{7}$$

Spherically symmetric Ansatz

In order to find a spherically symmetric solution, we consider the following Ansatz for the line element:

$$ds^2 = -e^{\Gamma(r)}dt^2 + e^{\Lambda(r)}dr^2 + r^2 d\theta^2 + r^2 \sin^2\theta d\varphi^2. \tag{8}$$

We also consider the Ansatz for a stationary and spherically symmetric scalar fields:

$$\Phi(r,t) = \phi(r)e^{-i\omega t} \text{ and } \psi = \psi(r), \tag{9}$$

where ω is the frequency of the field. We perform a rescaling of the parameters to simplify the equations:

$$r = \frac{\tilde{r}}{mv}, \quad \psi = v\tilde{\psi}, \quad \phi = v\tilde{\phi}, \quad \omega = mv\tilde{\omega}, \quad \kappa = \frac{\tilde{\kappa}}{v}, \quad \mu = m\tilde{\mu}. \tag{10}$$

Static Boson Stars in the E-FLS theory

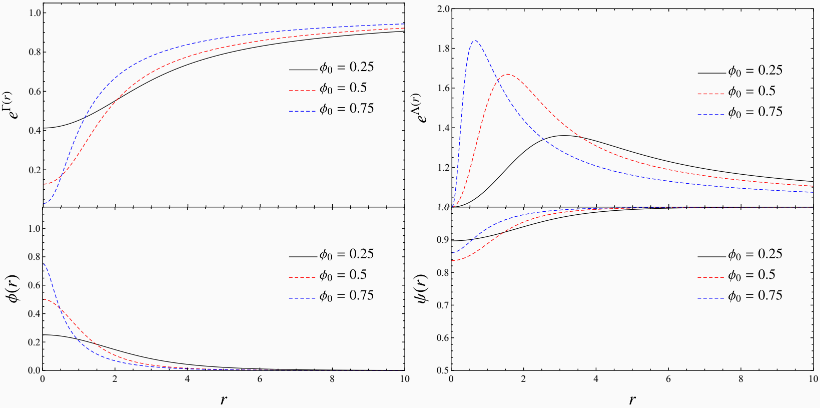

Figure 1: Numerical solutions for E-FLS stars with $\mu = 0.2$ and varying ϕ_0.

3. Astrophysical Images of E-FLS Stars

Astrophysical Images of E-FLS Stars

We compute the astrophysical images for four different E-FLS star configurations surrounded by geometrically thin accretion disks.

Table 1: Four distinct E-FLS star solutions and their properties.

Configuration	μ	ω	M	Number of light rings	r_+
FLS1	0.2	0.8873	0.5523	0	–
FLS2	0.2	0.8280	0.3715	2	0.0794
FLS3	0	0.8323	0.5043	0	–
FLS4	0	0.7828	0.3855	2	0.0896

Astrophysical Images of E-FLS Boson Stars

Assuming that the beam of photons are unpolarized, the radiative transfer equation is given by Lindquist in (Lindquist, 1966).

$$\frac{d}{d\lambda}\left(\frac{I_\nu}{\nu^3}\right) = \frac{j_\nu}{\nu^2} - \nu\,\alpha_\nu\,\left(\frac{I_\nu}{\nu^3}\right), \tag{11}$$

where I_ν, j_ν and α_ν are the specific intensity, emission coefficient and absorption coefficient, respectively. These quantities are measured by an observer comoving with the accretion disk. They are related to the invariant quantities, i.e. observer independent objects, as follows:

$$\mathcal{I} = \frac{I_\nu}{\nu^3}, \quad \eta = \frac{j_\nu}{\nu^2}, \quad \chi = \nu\,\alpha_\nu, \tag{12}$$

where ν is the frequency of the emission.

Geometrically thin and optically thick accretion disk

- **Geometrically thin and optically thick accretion disk**

For a geometrically thin and optically thick accretion disk, the solution for the radiative transfer equation (11). We consider that the accretion disk's emission is monochromatic with frequency ν_{em}:

$$I_\nu \propto \delta(\nu - \nu_{em})\, \epsilon(r), \tag{13}$$

as measured by an observer comoving with the accretion disk. Moreover based on (Rosa, 2022) and (Sengo, 2024), we assume that $\epsilon(r)$ behaves as follows:

$$\epsilon(r) \equiv \frac{1 + \tanh[50(r - 6M)]}{2} \left(\frac{6\,M}{r}\right)^3 . \tag{14}$$

The specific intensity as measured by the observer can be obtained from the invariant intensity (12), namely

$$I_{\nu'}^{obs} = \frac{\nu'^3}{\nu^3} I_\nu, \tag{15}$$

where ν' is the observed frequency.

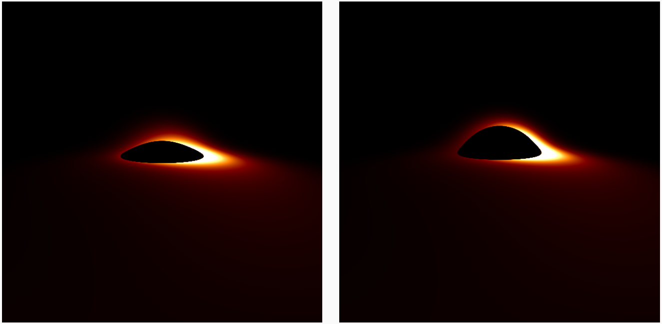

Figure 2: The intensity maps for FLS1 and FLS4 configurations, presented in Table 1, surrounded by an optically thick accretion disk. In this figure, we have positioned the observer at $r_{obs} = 20\,M$, $\theta_{\rm obs} = 80^{\circ}$, i.e., the observer is slightly displaced from the equatorial plane.

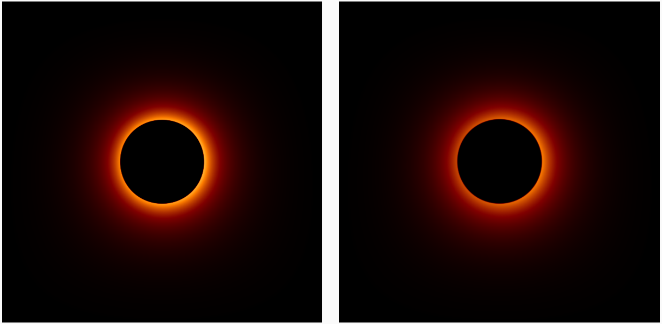

Figure 3: The intensity maps for FLS1 and FLS4 configurations, presented in Table 1, surrounded by an optically thick accretion disk. In this figure the observer is placed at $r_{obs} = 20\,M$, $\theta_{\rm obs} = 5^\circ$, i.e. the observer is close to a face-on observation of the accretion disk.

Astrophysical Images of E-FLS stars surrounded by an optically thin disk

- **Geometrically thin and optically thin accretion disk**

An optically thin disk is transparent to radiation and the light rays can cross it several times before being scattered. Each time that a given light ray intersects the accretion disk, it acquires more intensity. We consider the same emission profile as given in Eqs. (13)-(14). We also keep the position of the observer at $r_{obs} = 20\,M$ and vary the polar angle of observation.

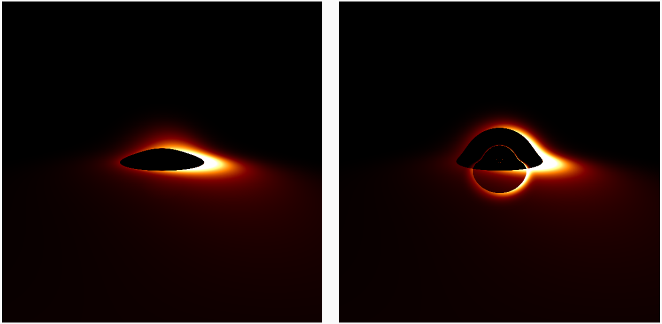

Figure 4: The intensity maps for the FLS1 and FLS4 configurations, presented in Table 1, surrounded by an optically thin accretion disk. Similarly to Fig. 2, we have positioned the observer at $r_{obs} = 20\,M$, $\theta_{\rm obs} = 80^{\circ}$.

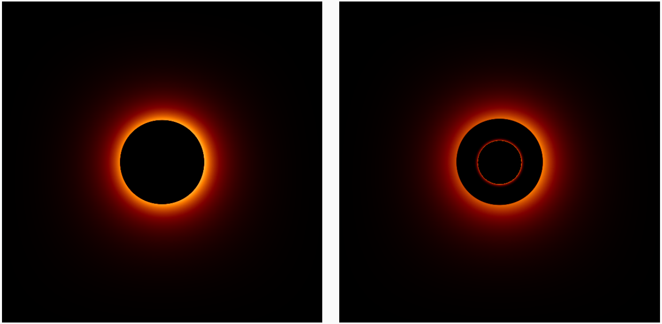

Figure 5: The intensity maps for FLS1 and FLS4 configurations, presented in Table 1, surrounded by an optically thin accretion disk. Similarly to Fig 3, we have positioned the observer at $r_{obs} = 20\,M$, $\theta_{\rm obs} = 5^\circ$.

4. Conclusion

- Decreasing the mass parameter μ modifies the E-FLS star features.
- The E-FLS stars support the presence of light rings and therefore more complex astrophysical images.
- In the present results, the light ring signature appears in the case of an optically thin accretion disk.

Acknowledgments

Acknowledgments

UNIVERSIDADE FEDERAL DO PARÁ

PPGF/UFPA

CAPES

universidade de aveiro

Grav@Zon

Bibliography

R. Friedberg, T. D. Lee and A. Sirlin, Class of scalar-field soliton solutions in three space dimensions. Phys. Rev. D **13**, 2739 (1976).

R. W. Lindquist, Relativistic transport theory. Annals of Physics, **37**, 487 (1966).

J. L. Rosa and D. R. Garcia, Shadows of boson and Proca stars with thin accretion disks. Phys. Rev. D **106**, 084004 (2022).

I. Sengo, P. V. P. Cunha, C. A. R. Herdeiro and E. Radu, The imitation game reloaded: effective shadows of dynamically robust spinning Proca stars. arXiv:2402.14919 (2024).

J. Kunz, I. Perapechka, and Y. Shnir, Kerr black holes with synchronised scalar hair and boson stars in the Einstein-Friedberg-Lee-Sirlin model. JHEP **07**, 109, (2019).

J. Kunz, V. Loiko, and Ya. Shnir, $U(1)$ gauged boson stars in the Einstein-Friedberg-Lee-Sirlin model. Phys. Rev. D **105**, 085013, (2022).

C. Herdeiro, E. Radu, and E. dos Santos Costa Filho, Proca-Higgs balls and stars in a UV completion for Proca self-interactions. JCAP **05**, 022 (2023).

U. Ascher, J. Christiansen, and R. D. Russell, A collocation solver for mixed order systems of boundary value problems. Math. Comput. **33**, 659 (1979).

W. H. Press, S. A. Teukolsky, W.T. Vetterling. *Numerical recipes in C++: The art of scientific computing* (Cambridge University Press, 2002).

P. V. P. Cunha, E. Berti and C. A. R. Herdeiro, Light-Ring Stability for Ultracompact Objects. Phys. Rev. Lett. **119**, 251102 (2017).

A. Levin and V. Rubakov, Q-Balls with scalar charge. Mod. Phys. Lett. A **26**, 409 (2011).

V. Loiko, I. Parapechka and Ya. Shnir, Q -balls without a potential. Phys. Rev. D **98**, 045018 (2018).

- M. Y. Khlopov, B. A. Malomed, Y. B. Zeldovich, Gravitational instability of scalar fields and formation of primordial black holes. Mon. Not. R. Astron. Soc. **215**, 575 (1985).
- P. V. P. Cunha and C. A. R. Herdeiro, Stationary Black Holes and Light Rings. Phys. Rev. Lett. **124**, 181101 (2020).
- P. V. P. Cunha, J. A. Font, C. A. R. Herdeiro, E. Radu, N. S. Gual and M. Zilhão, Lensing and dynamics of ultracompact bosonic stars. Phys. Rev. D **96**, 104040 (2017).
- A. Bohn, W. Throwe, F. Hbert, K. Henriksson, and D. Bunandar, What does a binary black hole merger look like? Classical Quant. Grav. **32**, 065002 (2015).
- P. V. P. Cunha and C. A. R. Herdeiro, Shadows and strong gravitational lensing: a brief review. Gen. Relativ. Gravit. **50**, 42 (2018).

H. C. D. Lima Junior, P. V. P. Cunha, C. A. R. Herdeiro, and L. C. B. Crispino, Shadows and lensing of black holes immersed in strong magnetic fields. Phys. Rev. D **104**, 044018 (2021).

C. W. Misner, K. S. Thorne and J. A. Wheeler, Gravitation (Freeman, San Francisco, 1973).

S. E. Gralla, D. E. Holz and R. M. Wald, Black hole shadows, photon rings, and lensing rings. Phys. Rev. D **100**, 024018 (2019).

M. D. Johnson *et al.*, The Black Hole Explorer: Motivation and Vision. arXiv:2406.12917 (2024).

M. D. Johnson *et al.*, Key Science Goals for the Next-Generation Event Horizon Telescope. Galaxies **11**, 61 (2023).